

THE CARBOEUROPE REGIONAL EXPERIMENT STRATEGY

BY A. J. DOLMAN, J. NOILHAN, P. DURAND, C. SARRAT, A. BRUT, B. PIGUET, A. BUTET, N. JAROSZ, Y. BRUNET, D. LOUSTAU, E. LAMAUD, L. TOLK, R. RONDA, F. MIGLIETTA, B. GIOLI, V. MAGLIULO, M. ESPOSITO, C. GERBIG, S. KÖRNER, P. GLADEMARD, M. RAMONET, P. CIAIS, B. NEININGER, R. W. A. HUTJES, J. A. ELBERS, R. MACATANGAY, O. SCHREMS, G. PÉREZ-LANDA, M. J. SANZ, Y. SCHOLZ, G. FACON, E. CESCHIA, AND P. BEZIAT

Models and observational strategies of carbon exchange need to take into account synoptic and mesoscale transport for correct interpretation of the relation between surface fluxes and atmospheric concentration gradients.

Adequate quantification of the geographical distribution of sources and sinks of CO₂ is still a major task with considerable implications for both our understanding of the global climate and the possible opportunities to mitigate climate change. Atmospheric measurements of CO₂ mixing ratios at a number of locations around the globe have helped significantly to quantify the source–sink distribu-

tion of carbon at the global and subhemispheric scales (e.g., Rödenbeck et al. 2003). The techniques that achieve this (e.g., Gurney et al. 2002) use a globally distributed network of atmospheric concentration observations together with an atmospheric transport model that back calculates an “optimal” source–sink distribution. This inverse modeling technique requires considerable a priori informa-

AFFILIATIONS: DOLMAN, TOLK, AND RONDA—Department of Hydrology and Geoenvironmental Sciences, Vrije Universiteit Amsterdam, Amsterdam, Netherlands; NOILHAN, SARRAT, BRUT, AND PIGUET—Météo-France, CNRM/GMME, Toulouse, France; DURAND—Laboratoire d’Aérodynamique, Université Paul Sabatier, Toulouse, France; BUTET—SAFIRE, CNRS-INSU, Météo-France, CNES, Toulouse, France; JAROSZ, BRUNET, LOUSTAU, AND LAMAUD—INRA, EPHYSE, Bordeaux, France; MIGLIETTA AND GIOLI—CNR IBIMET, Florence, Italy; MAGLIULO AND ESPOSITO—CNR ISAFoM, Naples, Italy; GERBIG AND KÖRNER—Max Planck Institute for Biogeochemistry, Jena, Germany; GLADEMARD, RAMONET, AND CIAIS—Laboratoire des Sciences du Climat et de l’Environnement, Gif sur Yvette, France; NEININGER—METAIR, Hausen am Albis, Switzerland; HUTJES AND ELBERS—Alterra, Wageningen, Netherlands; MACATANGAY AND SCHREMS—University of Bremen, Bremen, Germany; PÉREZ-LANDA

AND SANZ—CEAM, Valencia, Spain; SCHOLZ—Institut für Energiewirtschaft und Rationelle Energieanwendung, University of Stuttgart, Stuttgart, Germany; FACON—CNES, Toulouse, France; CESCHIA AND BEZIAT—CESBIO, Toulouse, France

CORRESPONDING AUTHOR: Dr. A. J. Dolman, Department of Hydrology and Geoenvironmental Sciences, Vrije Universiteit Amsterdam, Boelelaan 1085, 1081 HV, Amsterdam, Netherlands
E-mail: han.dolman@geo.falw.vu.nl

The abstract for this article can be found in this issue, following the table of contents.

DOI:10.1175/BAMS-87-10-1367

In final form 27 April 2006
©2006 American Meteorological Society

tion on the assumed source–sink initial patterns, their correlations, and errors. Unfortunately, so far, the global inversion approach yields estimates that are not robust beyond the (sub) continental scales (Gurney et al. 2002). In contrast, at the local scale (1 km²), direct flux measurements by eddy covariance (EC) techniques (Valentini et al. 2000) constrain the Net Ecosystem Exchange (NEE) to within 20%, comparable to the uncertainty estimated from inverse models (e.g. Janssens et al. 2003). In parallel, intensive field studies can determine the changes in vegetation and soil carbon stocks using biometric and inventory techniques, which allow independent quantification of the average carbon balance of ecosystems, be it also with significant uncertainties (Curtis et al. 2002).

These two scales, the global and the local, meet at the regional scale. However, how precisely these two scales interact at the regional level is unknown, and it remains a major challenge—both politically in the Kyoto context and scientifically—to quantify the carbon balance at this “missing scale.” The crucial breakthrough in understanding the sub-continental-scale carbon cycle may come when plot level measurements of fluxes and inventories can be aggregated and upscaled in such a way that they match the observed CO₂ concentration or the predictions from inverse models at high spatial resolution. Such a breakthrough requires an understanding of both the role of regional meteorology and land management practices in regulating the fluxes from the land to the atmosphere. This knowledge can be obtained with high-intensity experimental campaigns (e.g. Schmitgen et al. 2004; Gerbig et al. 2003; Dolman et al. 2005). This paper describes such an experimental campaign.

The CarboEurope Regional Experiment Strategy (CERES; see also <http://carboregional.mediasfrance.org/index>) aimed to produce aggregated estimates of the carbon balance of a region that can be meaningfully compared to those from the smallest downscaled information of atmospheric measurements and continental-scale inversion results. The key challenge in this experiment is to obtain atmospheric data at high spatial and temporal resolution that can be used to extract information of the surface carbon exchange at similar high resolution. In May–June 2005 we executed a strategically focussed regional field experiment in Les Landes, southwest France, to obtain this data. If successful, this will not only lay the foundation for implementing a year-long campaign for 2007 with reduced experimental effort, but also for a similar continuous observation network across Europe in the future. It will also allow for integrating carbon obser-

vations of a different nature such as eddy covariance fluxes, plot- and regional-scale inventories, remote sensing, and atmospheric concentrations. Above all, it will improve our process understanding of the major controls of the emission and uptake of CO₂ at the regional scale. At the global scale such process understanding is often difficult to obtain.

In the past, several regional studies of the carbon fluxes have been conducted, either predominantly based on ground level data and remote sensing [e.g., Hydrological Atmospheric Pilot Experiment–Modélisation du Bilan Hydrique (HAPEX–MOBILHY), André et al. 1986; First International Satellite Land Surface Climatology Project (ISLSCP) Field Experiment (FIFE), Sellers et al. 1988; Boreal Ecosystem–Atmosphere Study (BOREAS), Hall 2001], or alternatively focused on atmospheric sampling [e.g., CO₂ Budget and Rectification Airborne study (COBRA), Gerbig et al. 2003; Cooperative LBA Airborne Regional Experiment (LBA–CLAIRE–98), Andreae et al. 2001]. Gioli et al. (2003), Schmitgen et al. (2004), and de Arellano et al. (2004) describe elements of several pilot experiments that were performed in the framework of the CarboEurope cluster project Regional Assessment and Modelling of the Carbon Balance of Europe (RECAR). Based on experience from those studies, the regional experiment CERES was planned to combine various types of ground-based carbon cycle–related measurements and atmospheric observations with remote sensing to infer a regional carbon budget.

EXPERIMENTAL STRATEGY. The scaling problem between local and global carbon balance studies becomes clearer if one appreciates how large-scale inversion-based sink–source estimates, obtained by a limited number of observations, suffer from a number of errors (e.g., Gerbig et al. 2003). First, measurements from a single location are not necessarily representative of larger regions or model grid cells (“representation errors”). Second, solving for fluxes that do not evenly influence the overall concentration may cause “aggregation errors” (Kaminski et al. 2001). Finally, diurnal and seasonal fluctuations in the boundary layer heights that cause the CO₂ concentration to co-vary with the fluxes are usually poorly represented in large-scale transport models, and cause “rectification errors” (Denning et al. 1996). CERES aimed to obtain the data that would better allow quantifications of these errors.

The central methodology of CERES is to make concentration measurements both within and above the boundary layer and to couple those via a model-

ing/data assimilation framework to the flux measurements at the surface and within the boundary layer. To achieve this, we instrumented a region near Les Landes forest with ground- and air-based measurements at high spatial and temporal resolution. This area was chosen because of the wealth of supporting data that exist from the previous HAPEX–MOBILHY experiment (André et al. 1986) and the vicinity of Météo-France in Toulouse with state-of-the-art forecasting tools. Such a multiple constraint approach has not been tried before at the regional level and the data are thought to give a better understanding of the surface source–sink distributions and allow for a better quantification of the errors listed above.

Description of the experimental area. The experimental domain covers an area of about 250 km × 150 km in southwest France. It is bounded to the west by the Atlantic Ocean, the shoreline being almost rectilinear along a north–northeast orientation. The western half of the domain is dominated by Les Landes forest, of which 80% is included in the Regional Experiment area (Fig. 1). The forest is mainly composed of maritime pines (*Pinus pinaster* Ait.). It is a plantation forest that was originally planted to drain the marshlands, managed as a commercial forest, with regular harvests and rotation. There are clearings of various size, which contain agricultural land, mainly maize, but also grassland and pasture (in the southern part of the forest), or other cultivars like vegetables. Close to the west coast, some large ponds can be found. Most of this land is covered by cereals, such as maize, with the exception of the Garonne River valley (crossing the domain from southeast to northwest) where there are fruit trees, and the large “Bordeaux” vineyards, east and northwest of Bordeaux city. There are mostly winter crops towards the southeast, whereas summer crops increase toward Les Landes forest.

The northeast corner is a vast, little-cultivated region, mainly composed

of woods and pastures. Two major cities are located close to the southeast (Toulouse) and northwest (Bordeaux) corners of the domain. A little less than one million inhabitants live in Toulouse and its suburbs, about one and a half times that of Bordeaux. Given the dominant winds in spring, the domain could be affected by the plumes of the cities. The population of the other cities inside the domain is an order of magnitude lower than that of Toulouse or Bordeaux.

Les Landes forest and the valley of the Garonne River are relatively flat areas, whereas the rest of the domain is mainly composed of gentle hills. Outside the domain, to the south, the Pyrénées mountain range presents a solid west–east barrier rising occasionally above 3000-m height. This has a strong influence on the generation of local winds in the domain. To the east and northeast, the terrain elevates progressively toward the Massif Central, culminating at 1800 m and reaching about 1000 m, 100 km from the domain.

Deployment of instrumentation. We installed a set of ground-based surface flux measurements, regular radiosoundings, and wind and temperature profilers and performed aircraft measurements with low-flying flux aircraft. We also performed boundary layer sampling with small aircraft and flew long

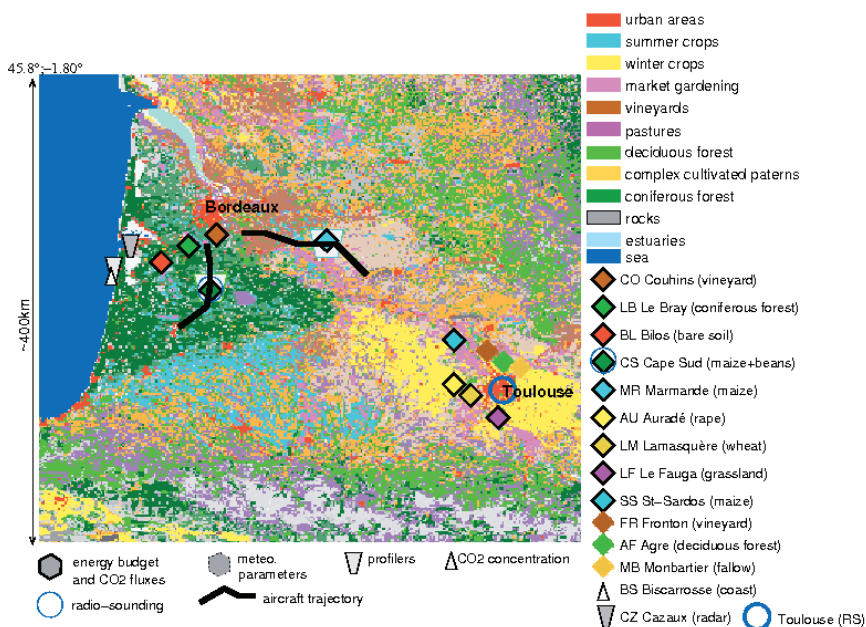


FIG. 1. Land cover map at 250-m resolution for the experimental domain in the southwest region of France showing the different locations of summer and winter agricultural crops (classification by Champeaux et al. 2005). Also shown are the locations of the ground-based observation sites of surface fluxes and boundary layer. Flight tracks indicate the path flown by the Sky Arrow flux aircraft for agriculture and forested regions.

trajectories with two research aircraft. Figure 1 shows how the ground-based instruments were deployed geographically. Climatic analysis suggested that dominant winds would be either from the west or the east; therefore, we expected to be able to observe modification of the CO₂ concentration profiles by the land as the air mass progressed east- or westward. Our design was based on capturing this phenomenon with continuous CO₂ concentration measurements on towers near the coast and inland, with several flux towers scattered in between to sample the different land cover types.

Ground-based measurements. At the coastal boundary of the domain, near Biscarrosse France, (Fig. 1), a high-precision CO₂ instrument, called the CARIBOU, was installed on a 40-m tower. The accuracy of the CO₂ concentration measurement is of the order of 0.1 ppm. We also deployed a 20-m tower near Marmande France, (Fig. 1) with a new low cost device for continuous CO₂ monitoring with intermediate accuracy. In a half-hour cycle up to six levels can be sampled. Twice a day, at noon and midnight, a CO₂ calibration gas sample is measured by the analyzer to allow a postcorrection on the concentrations. Accuracy, after the calibration correction is applied, is better than 1-ppm CO₂. This accuracy is lower than provided by the CARIBOU system, but because of the large diurnal concentration fluctuations, we hope that the data are of sufficient quality to be used in high-resolution atmospheric model inversions.

Fluxes of water, energy, and CO₂ were measured using the eddy correlation technique. The basic instruments and methods have been standardized throughout the Euroflux and CarboEurope ecology network (Aubinet et al. 2000). The EC system consists of a 3D sonic anemometer coupled with open or closed path CO₂/H₂O InfraRed Gas Analyzers (IRGA). Measurements were obtained above eight different land covers: a vineyard, a pine forest, a clear-cut forest where pine trees have just been resown, maize (three sites), beans, rape, grassland, and above a wheat surface. Table 1 gives an overview of the sites and variables measured.

At three sites (Cape Sud, Marmande, and routinely near Cazaux) we obtained continuous information on the wind field within the boundary layer through two UHF and sodar profilers. The sodar system near Marmande was extended with a radio acoustic sounder unit to obtain information on the temperature profile of the lower boundary layer, typically up to 500–700 m. At Cape Sud we also installed a modified ceilometer laser to detect the height of the boundary layer.

Near Biscarrosse we also obtained Fourier transform infraRed (FTIR) measurements of column abundances for a number of trace gases, including CO₂. These measurements are very useful for future validation of remotely sensed column concentrations of greenhouse gases, and the collocation at Biscarrosse with the high-precision measurement provides an opportunity to assess the performance of the instrument. The measurement principle of FTIR is based on the characteristic wavelengths of absorption of trace gases. This allows retrieving column densities of several tropospheric and stratospheric gases such as CO₂, CH₄, CO, N₂O, C₂H₂, C₂H₆, CH₂O, OCS, and various CFCs.

From a site in Les Landes, Cape Sud, radiosondes were launched at 3-hourly intervals during the intensive observation periods (IOPs), while at Toulouse on special days an extra sonde was launched at 1200 UTC. All the profiles taken at 0500, 1100, 1700, and 2300 UTC were sent immediately to the operational weather data system and incorporated into the limited-area weather assimilation scheme to improve the quality of the analyzed and forecast fields in the area. Special constant volume balloons were launched from Cape Sud at particular occasions to sample the atmosphere's temperature and moisture in truly Lagrangian fashion at fixed density levels. The information of the wind patterns and flight path of the balloon was transmitted on some occasions to the pilot of the aircrafts to help them fly in Lagrangian air sampling mode.

Airborne measurements. The advent of small specialized airplanes in the past decade, measuring fluxes at a resolution of a few kilometers and with comparable accuracy to tower fluxes, has greatly increased the possibilities to provide accurate estimates of fluxes in areas of substantial spatial heterogeneity (Crawford et al. 1996; Gioli et al. 2003). The Sky Arrow, a low- and slow flying aircraft, equipped with a state-of-the-art mobile flux platform to measure fluxes of CO₂, heat, water vapor, and momentum, was used in the current experiment. We had two Sky Arrows available, with one equipped with a multispectral scanner that was used to obtain high-resolution Normalized Difference Vegetation Index (NDVI) images. The other Sky Arrow flew flux transects among the forest and agricultural areas, typically at 50–100 m above the canopy.

The Piper Aztec (PA23-250) belonging to Météo-France performed continuous measurements of CO and meteorological variables and was equipped with the CONDOR instrument to measure CO₂ concentrations in situ at high accuracy. The CONDOR is based

TABLE 1. Summary of ground flux sites with variables observed during the full campaign. Abbreviated site names and location can be found on Fig. 1.

| Parameter | Site | | | | | | | | | | | | | | | |
|-----------------|----------------------|----|----|----|--------------------|--------------------|----|----|----|----|----|----|----|----|----|---|
| | BS | CZ | BL | LB | C _{maize} | C _{beans} | CO | MR | FR | AF | MB | SS | LF | AU | LM | |
| Meteorology | Pressure | | • | • | • | | | • | • | • | • | • | • | • | • | |
| | Temperature | • | • | • | • | • | • | • | • | • | • | • | • | • | • | |
| | Canopy temperature | | | | | | | | | | | | | | • | • |
| | Moisture | • | • | • | • | • | • | • | • | • | • | • | • | • | • | • |
| | Incoming radiation | | • | • | • | • | • | • | • | • | • | • | • | • | • | • |
| | Light interception | | | | | | | | | | | | | | • | • |
| | Net radiation | | | • | • | • | • | • | • | • | • | • | • | • | • | • |
| | Wind | • | • | • | • | • | • | • | • | • | • | • | • | • | • | • |
| | Rain | • | • | • | • | • | • | • | • | • | • | • | • | • | • | • |
| CO ₂ | Concentration | • | | • | • | • | • | • | | | | • | • | • | • | |
| | PPFD* | | | • | • | • | | • | | | | | | • | • | |
| | Soil emission | | | | | | | | | | | | | • | • | |
| Soil | Temperature | | | • | • | | • | | • | • | • | • | • | • | • | |
| | Moisture | | | • | • | | • | | • | • | • | • | • | • | • | |
| | Soil heat flux | | | • | • | | • | | | | | • | • | • | • | |
| | Sensible heat flux | | | • | • | • | • | • | • | | | • | • | • | • | |
| | Latent heat flux | | | • | • | • | • | • | • | | | • | • | • | • | |
| Eddy flux | Momentum flux | | | • | • | • | • | • | • | | | • | • | • | • | |
| | CO ₂ flux | | | • | • | • | • | • | • | | | • | • | • | • | |
| | Ozone flux | | | | | • | • | | | | | | | | | |
| | NO _x flux | | | | | | • | | | | | | | | | |

*Photosynthetic photon flux density.

on a commercial Non Dispersive Infra Red Analyzer (Li-COR 6262) equipped with a fast-response detector with a high acquisition frequency (1 Hz) that has turned it into a dedicated tool for airborne measurements. This allows it to achieve an accuracy of typically 0.2 ppm. Moreover on board the Piper flask samples were taken for later analysis of trace gases (CO, CH₄, N₂O, and isotopes (C¹⁴ and C¹³)).

The second aircraft used for concentration measurements was the “ECO-Dimona” (DIMO) of MetAir, Switzerland. The DIMO is a small and versatile airborne measuring platform that can carry two underwing pods with scientific instruments. During CERES, the focus was on the concentrations of CO₂, CO, H₂O, and NO₂, and the 3D wind in turbulent resolution. For CO₂, three methods were in use: both a modified LI-6262 [closed path IRGA as described in Schmitgen et al. (2004) and a modified LI-7500

(open path IRGA with a new mounting)], plus up to 12 flask samples per flight (also for CO, other trace gasses, and isotopes). The combined accuracy (resolution) of this threefold system is 0.2 ppm (10 Hz). The absolute accuracy of the high-resolution water vapor measurements was supported by a dew-point mirror. Additional sensors that were in use were for O₃, NO_x, aerosols (number concentrations of >0.3 and >0.5 μm), and a downlooking hyperspectral scanner [350 to 1050 nm with a parallel-looking camera (1 averaged spectrum/photo every 0.7 s)]. Operationally, it was important that the crew (pilot plus scientist) could make ad hoc decisions based on real-time data, and input from the ground (e.g., results of nearby soundings).

There are two basic ways to sample the concentration of CO₂ in the atmosphere: Eulerian (grid based) and Lagrangian (air mass following). Information of

| TABLE 2. Summary of operations during IOPs. | | | | | | | | | | |
|---|---------------------------------------|--|---|-----------------|-----------------|---------------------|-----------------------------------|---|-----|---|
| IOP | Weather conditions | Aircraft operations | | | | Soundings | | | LB* | Remarks |
| | | Piper | DIMO | Sky Arrow flux | Sky Arrow RS*** | Toulouse (UTC) | Z ₁ ** (m) at 1700 UTC | LCS (UTC) | | |
| 18–20 May | Anticyclonic 19–20 May clear skies | 1 profile, 2 Les Landes 36 flasks | | 12 flux flights | | 19–20 May: 1100 | | 18 May: 6, 18 19–20 May: 5, 8, 11, 14, 17 | | Initial problems with CONDOR. Best day: 19 May |
| 23–27 May | Anticyclonic, clear skies, weak winds | 5 Les Landes, 1 Les Landes Toulouse, 72 flasks | 6 flights, mostly Lagrangian. 60 flasks | 10 flux flights | 4 RS flights | 24–27 May: 1100 | 1100–1900 | 23 May: 17 24–26 May: 5, 8, 11, 14, 17, 23 27 May: 5, 8, 11, 14, 17 | 4 | Intercomparison profiles flown. Best day: 27 May |
| 31 May–2 June | Fair weather, high clouds, NE-E winds | 2 Les Landes 18 flasks | | 6 flux flights | 3 RS flights | 31 May–2 June: 1100 | 1600–2000 | 31 May: 5, 11, 17, 23 1 June: 5, 8, 11, 14, 17, 23 2 June: 5, 11, 17 | | Best day: 1 June |
| 6–10 June | Anticyclonic weak winds W-NE to NE | 4 Les Landes and 1 Lagrangian 47 flasks | 2 Lagrangian 21 flasks | 12 flux flights | 6 RS flights | 6–10 June: 1100 | 1300–1800 | 6 June: 5, 8, 11, 14, 17 7 June: 5, 11, 14, 17, 23 8–9 June: 8, 11, 14, 17, 23 10 June: 5, 8, 11, 14, 17 | 7 | Intercomparisons and tracking of Bordeaux plume. Best days: 6, 8 June |
| 14–15 June | Westerly flow | 2 Lagrangian 18 flasks | 2 Lagrangian 24 flasks | | | 15–16 June: 1100 | 1000–1200 | 14 June: 5, 8, 11, 14, 17 15 June: 5, 11, 14, 17 | | Best day: 15 June |
| 18–22 June | Anticyclonic very hot | 3 Les Landes 28 flasks | | 6 flux flights | 3 RS flights | | | 19 June: 5, 11, 17 | | Best day: 19 June |

*Lagrangian balloon.

**Height of the mixed layer.

***Remote sensing

the weather forecast and detailed trajectory modeling (e.g., Lin et al. 2003) were used to determine exact flight patterns. The footprint, or surface influence, for a given measurement time and location was derived with adjoint transport models that were driven by assimilated meteorological fields from the European Centre for Medium-Range Weather Forecasts (ECMWF) and Aladin (Météo-France) mesoscale weather analysis. The Stochastic Time Inverted Lagrangian Transport model (STILT) was used to extract this footprint information (Lin et al. 2003) so that up to five days in advance we could plan our flights.

Quality control and assessment. Special attention was given to obtain the CO₂ concentration measurements as reliably and accurately as possible. The CO₂ concentrations were measured at ground stations, on towers, and on board airplanes, both in situ and with flask samplings. Variations in CO₂ concentrations, as large as several tens of parts per million or even more, were observed both on horizontal distances of tens of kilometers or, at a given place, during the course of the day. Although the absolute accuracy of the various instruments is able to capture such variability, to calculate the CO₂ budgets at a time scale of a whole (or several) day(s) and over the whole area would require a much better accuracy because of the averaging involved. This is the reason why we executed a more precise quality control and quality assessment procedure. Given that the CARIBOU system (0.1 ppm), we calibrated our other instruments against this instrument on a single day toward the end of the campaign. On every profile performed by the Piper Aztec, three or four flasks were filled at various levels inside and above the bound-

ary layer, to a posteriori evaluate the functioning of the continuously measuring CONDOR system. A total of 110 flasks were used, the major part of them above the Marmande area [where the Radio Acoustic Sounding System (RASS) sodar was installed] or over the ocean, close to the shoreline where the CARIBOU system was set up. The DIMO aircraft also used 40 flasks to postcalibrate its closed-path Licor system. The Piper Aztec, Sky Arrow, and DIMO also flew several paired common profiles, above Marmande and/or Cape Sud. This full inter-comparison between all systems is currently underway. Finally, as for the eddy correlation calculations, each group used its own software, but for post-processing we decided to use single software to analyze all data, so as to provide a consistent analysis.

FIRST RESULTS. A 6-week period in the spring of 2005 (from 16 May 2005 to 25 June 2005) was chosen for high-intensity observations of boundary layer development and flux aircraft for enhanced spatial sampling. When the weather forecast and footprint modeling suggested good days for flying the aircraft, a so-called IOP was announced. Table 2 gives an overview of Intensive Observational Periods. During IOPs we attempted to fly as many instruments as we could, executed an intensive radiosonde program with launches at 0500, 0800, 1100, 1400, 1700, and 2300 UTC, and flew when possible one or two Lagrangian balloons. In total we obtained about 21 days of intensive measurements. Starting problems with the instrumentation meant that the first IOP contained

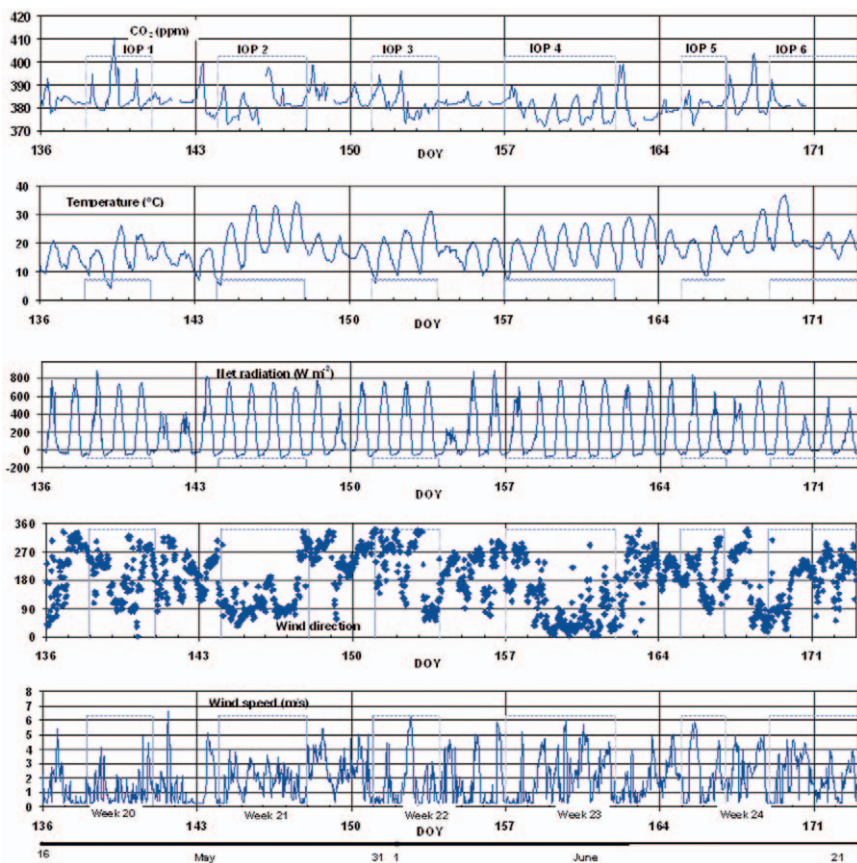


FIG. 2. Time series of (from top to bottom) CO₂ concentration, temperature, net radiation, wind direction, and wind speed observed near the Biscarrosse tower. Also shown are the periods when IOPs were held.

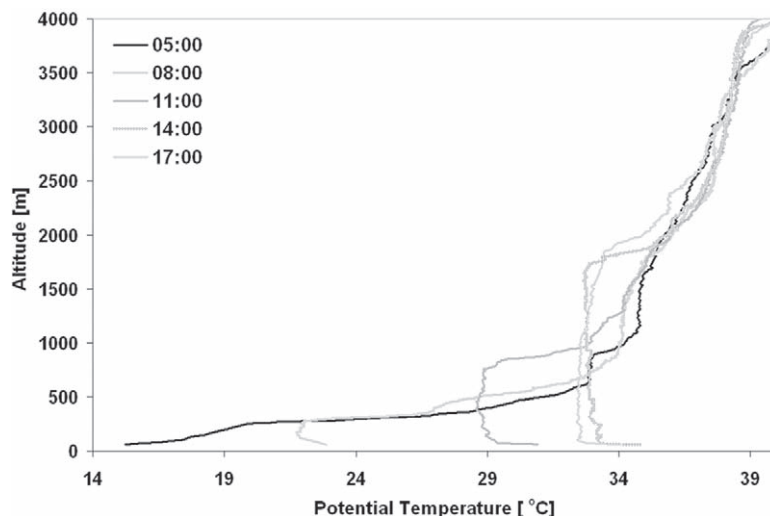
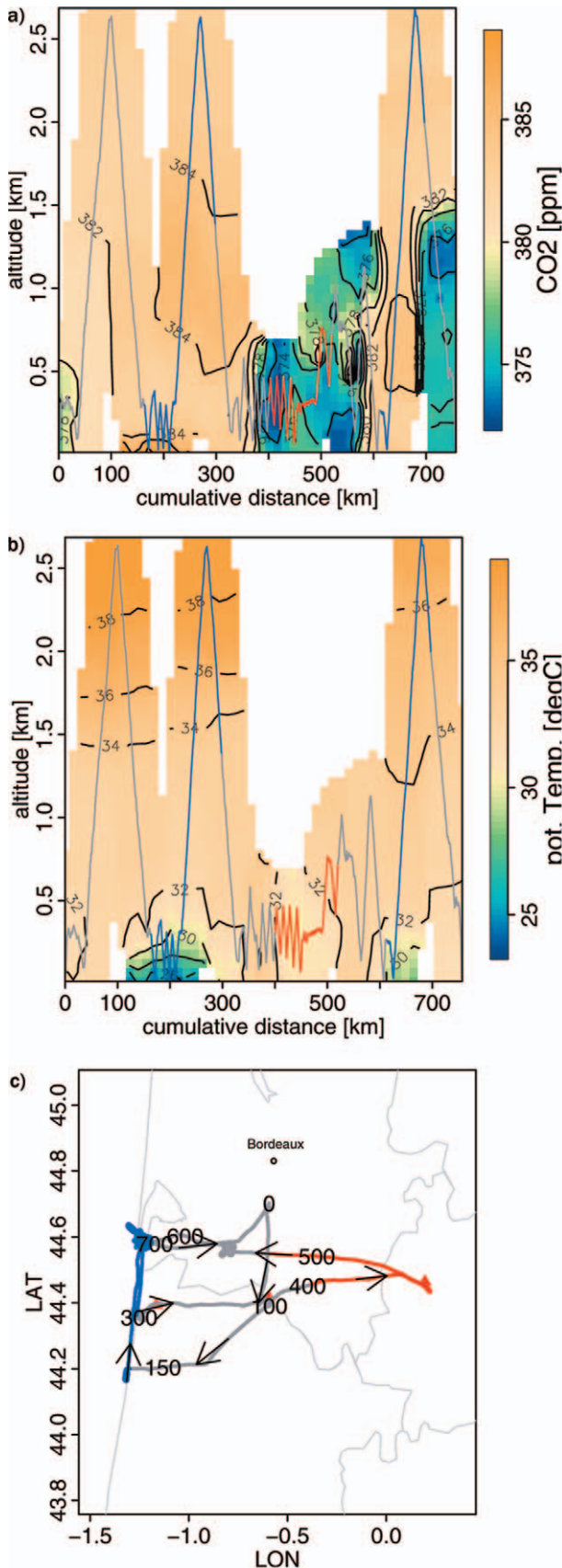


FIG. 3. Development of potential temperature on 27 May from the radiosondes launched at Cape Sud.

somewhat less data coverage than the later ones. Figure 2 shows the time series of CO₂ concentration at Biscarrosse and meteorological observations for the full experimental period, with the IOPs also indicated.



IOP-2. We present some preliminary results from the second IOP that lasted from 24 to 27 May. During this period there was a strong anticyclonic situation over the area with very weak variable winds. Figure 3 presents the boundary layer structure at Cape Sud during the last day of the IOP. Particularly noteworthy is the very deep (1.7 km) boundary layer that develops over the forest during the day. It is topped by a very sharp inversion that is accompanied by a strong humidity decrease (not shown), where above 1.7 km a very dry layer of air has developed. This high final boundary layer depth appears to be facilitated by a quick development through the residual boundary layer of the previous day in the early part of the afternoon.

Figures 4a,b show an image obtained from the DIMO flight on the afternoon of 27 May. Figure 4c shows the flight plan. The aircraft tried to intercept the constant volume balloon that was released, so as to obtain a perfect Lagrangian flight path. The main advantage of this type of sampling is that any changes in the air mass can be attributed directly to fluxes encountered by the air mass from the ground or overlying air, as it travels along its path. In Figs. 4a and 4b the concentration of CO_2 and temperature along the flight path are shown. The aircraft took off from Saucats airport, and flew south to intercept the balloon at release near Cape Sud, then westward to the coast, after which it flew south for 100 km then flew inland along a northeast line to Marmande. After Marmande it flew west toward the coast, intercepting the balloon. Carbon dioxide concentrations vary along the flight track from 375 to 385 ppm in the boundary layer, with the highest concentration close to the ocean surface. The lowest concentrations are observed over the agricultural area. Because the winds were weak and variable, we expect that most of this variation is related to different uptake and emission regimes of the land surface. If this is true, the agricultural areas in the east part of the flight would be a larger sink than the forest in the west. Our surface flux measurements over Les Landes forest for this day and the previous day show a relatively high uptake rate, while our flux station in Marmande shows small net CO_2 fluxes (see Fig. 5). These latter observations were obtained over an area of growing maize that had

FIG. 4. DIMO flight 27 May 2003. (a) Contour plot of CO_2 concentration against distance flown, (b) contour plot of potential temperature against distance flown, and (c) the flight track. Red color codings indicate agricultural (summer crops) areas; black, forested areas; and blue, the sand dunes of the coastline.

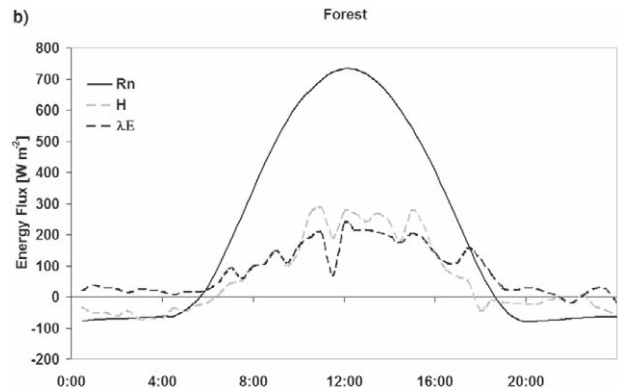
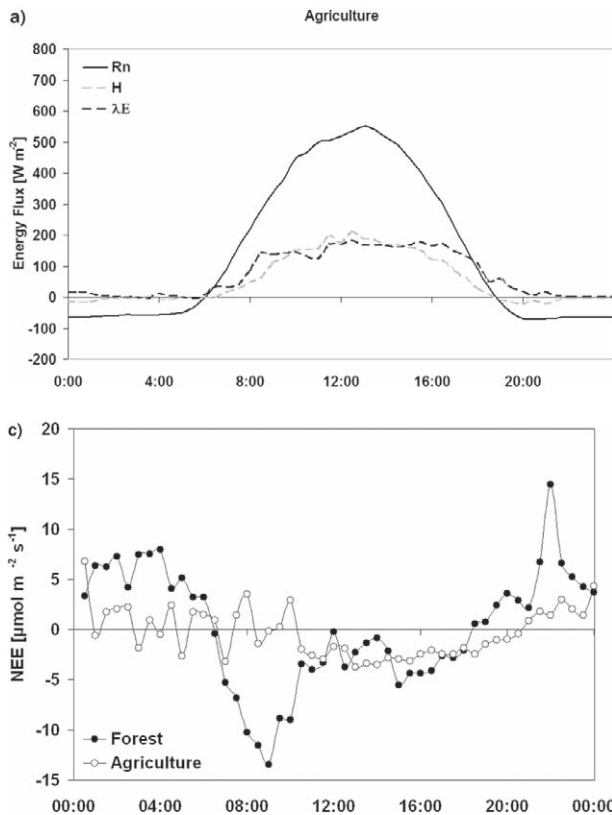


FIG. 5. Surface fluxes for 27 May 2005. (a) Net radiation, soil heat flux, and latent and sensible heat above the forest of Le Bray. (b) Net radiation and latent and sensible heat above maize in Marmande. (c) Fluxes of NEE above Le Bray in Les Landes forest and maize in Marmande.

large parts of soil exposed to the air and produced relatively high respiration. Our crop sites toward the southeast showed indeed fluxes of comparable magnitude as the forest fluxes. In fact, analysis of the land cover shows that toward the southeast of the domain the crops are predominantly winter crops that already have high CO₂ uptake rates, while the summer crops are still having low rates (Fig. 1).

The Sky Arrow measures latent and sensible heat, and this allows us to investigate the energy balance characteristics of the land surface at regional scale. Figure 6 shows the sensible heat, latent heat, and CO₂ flux at noon observed by the Sky Arrow. We show data from 24 May, because the flights above forest and agriculture were executed around the same time. On 27 May we do not have these nearly simultaneous flights available. Two things call for attention. The sensible heat flux over the forest is larger than that over the agricultural areas, whereas latent heat fluxes are more similar. At the agricultural areas the Bowen ratio is close to 1 during IOP-2, for the forests it is closer to 1.5. The high sensible heat flux above the forest is likely to be the major cause for the extremely high boundary layer depths observed during this day. The CO₂ fluxes over the forests are also much larger than in the agricultural areas, but comparable to those over the vineyards. Thus the

observed high concentration of CO₂ over the forest is not directly correlated with the flux, as the CO₂ flux is high, suggesting that the air over the forest area would be more depleted in CO₂ than observed. Latent heat flux correlates with the CO₂ flux over the forest but not over the agricultural area (Fig. 6b), suggesting that soil evaporation of arable land was contributing to the overall flux more than plant transpiration. In fact, areas planted with maize appear to act as a source of CO₂, as maize still is in the early stages of development at this time of the year.

The trajectories and footprints obtained by STILT may provide some further insight into this apparent discrepancy between fluxes and concentrations. Figure 7 shows the footprint calculations for the locations of Biscarrosse and Marmande using the Aladdin forecast for 1200 UTC 26 May. The footprint of Marmande is lying in a mostly westerly direction, in strong contrast to the Biscarrosse footprint that is strongly north–south oriented. In fact, the air sampled by the DIMO over Les Landes forest suggests that CO₂-rich air is advected northward along the coast, while air sampled near Marmande is strongly depleted in CO₂ because it moved over active vegetation areas in the southeast. Taking either the concentration at Biscarrosse or Marmande as representative of local fluxes, or taking the flux measurements at those sites as representative of large regions, would thus lead to incorrect conclusions. Clearly joint consideration of the synoptic and regional flow, fluxes, and land surface is required for a correct interpretation. The significant difference of the Biscarrosse to the Marmande footprint, given that the distance is only

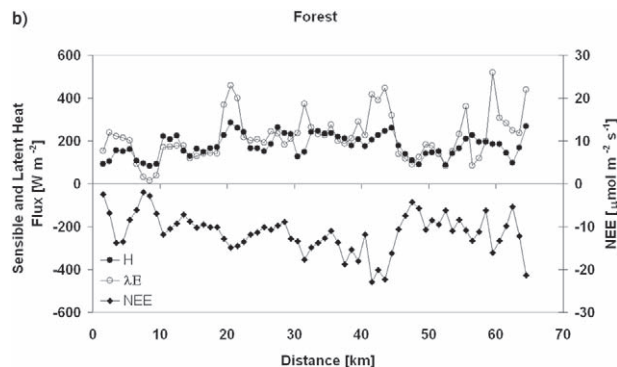
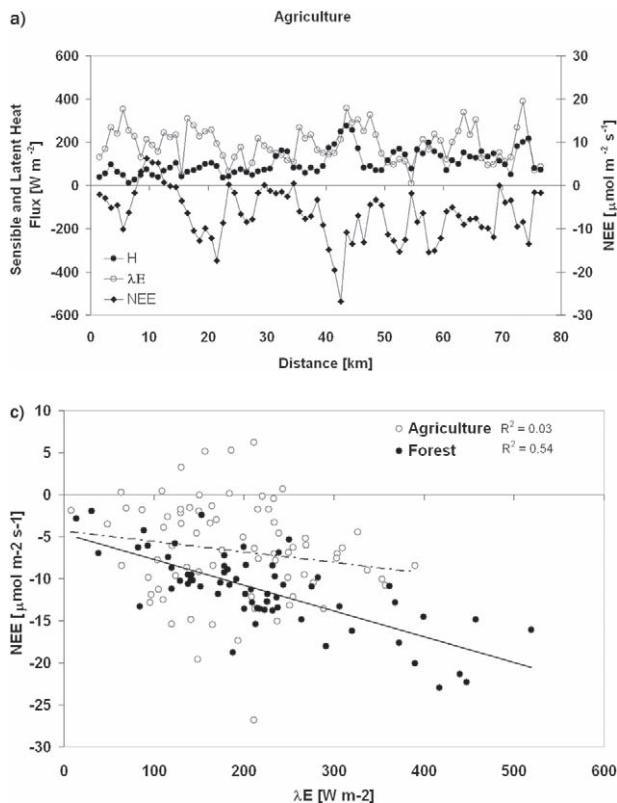


FIG. 6. Sky Arrow observations of 24 May 2005: fluxes of sensible and latent heat and CO₂ observed at 50–100-m altitude (a) over the forests and (b) over the agricultural area. The fluxes are not yet corrected for flux divergence. (c) The relation between CO₂ flux and evaporation for the agricultural and forest areas.

100 km, indicates a high variability of the synoptic flow that requires mesoscale modeling to properly resolve the observed tracer gradients. This was what CERES aimed to achieve.

The data obtained during CERES are not only suited for three dimensional interpretation, but because we applied several novel techniques, we also collected data that are very useful for furthering our process level understanding, such as the FTIR near Biscarosse and inexpensive concentration measurements (Marmande tower).

LESSONS LEARNED. CERES has provided a wealth of data that on its own could prove useful, but should be particularly useful as a comprehensive dataset to narrow down uncertainties in regional carbon balance estimation. It provides considerable insight into the large variability of spatial CO₂ fields (10–20 ppm over 200 km) and the strong diurnal range in the boundary layer that can approach 100 ppm as observed during night at the Marmande tower. The interpretation of these data requires insight into the synoptic-scale variation of boundary layer properties and flow patterns. Without appreciation of this 3D context of the relation between surface fluxes and atmosphere we could not understand some of the patterns we observed from the aircraft. It is ex-

actly this 3D context that has limited the usefulness of 1D inversions such as the convective boundary layer technique (Styles et al. 2002; Lloyd et al. 2001; Laubach and Fritsch 2002).

Atmospheric mesoscale models have been used as powerful tools to study regional exchange of water and energy (Noilhan and Lacarrère 1995). This development has been further taken up in CarboEurope, so that nonhydrostatic mesoscale models are now used to simulate the surface–atmosphere exchange of CO₂ at resolutions comparable to that of flux aircraft and single flux towers (e.g., 1–2 km). For such limited area transport models, the boundary conditions come from atmospheric coarser-scale models used in the Continental Integration Component (www.carboeurope.org). CERES intends to use both forward and backward modeling tools to simulate the CO₂ fields as well as estimate the regional source and sink distribution. During the execution of the experiment the availability of the Meso-NH model (Belair et al. 1998), running operationally without CO₂ fields, assisted already in adjusting flight plans depending on the predicted boundary layer heights and wind fields of the model.

Inversive methods for determining surface CO₂ fluxes have been used in first attempts at high-resolution regional scales both in the United States and in Europe (see, e.g., Gerbig et al. 2003; Lin et al. 2004; Ronda et al. 2006, manuscript submitted to *Atmos. Chem. Phys. Disc.*). For a previous CarboEurope winter campaign in the Netherlands, for instance, we were able to considerably decrease the uncertainty in regional fossil fuel emissions, indicating not only the strength of the method, but also its

usefulness to check fossil fuel emission inventories. Good transport models, however, are fundamental to the success in inversions of the concentration observations to obtain sink–source distributions (Peylin et al. 2002). The data of the boundary layer soundings and profilers will be extremely useful to quantify possible errors in the transport or structure of the boundary layer. This is an essential difference from the global-scale synthesis inversion methods that have been used in the past, since in the regional models development and structure of the boundary layer play key roles in determining the diurnal and spatial variation in CO₂ concentrations. Initial comparisons with Meso-NH output suggest that the modeled boundary layer depths compared well with our observations. We have started a model intercomparison for two days of the campaign, in which we will analyze model performance and further assess the capability of the mesoscale models to adequately represent transport at the mesoscale.

A further primary requirement to successfully use high-resolution mesoscale models for Bayesian CO₂ inversion of sources and sinks is the existence of accurate a priori flux distributions and high-resolution spatial and temporal distributions of fossil fuel sources. Such a high-resolution emission map was obtained by downscaling the regional estimates to 6-hourly time steps and 1-km resolution. Realistic mapping of the surface fluxes relies on information on land cover, and surface biophysical parameters [leaf area index (LAI) and albedo] that can be obtained from high-resolution (e.g., *Landsat*, *Spot*, and *Aster*) and high-repetitiveness (e.g., *Vegetatio*, *Modis*, *Meris*) spaceborne images. Because data were obtained of surface fluxes for a variety of land cover types, we expect to reduce uncertainties in flux parameterizations considerably. The atmospheric mesoscale transport models are fitted with land surface packages [soil–vegetation–atmosphere transfer (SVAT)] and are excellent tools to act as

a host platform for data assimilation of field and model data, similar to the use in, for instance, past field experiments like HAPEX–MOBILHY, which focused on water and energy exchange only (e.g., Bougeault et al. 1991). Estimating regional, subnational carbon exchange for protocol verification purposes also requires upscaling in time, as the carbon cycle is a combination of slowly interacting processes in soils and biomass with very fast ones in meteorology (e.g., Körner 2003). CERES so far has been mainly concerned with the fast interaction, but we wish to be able to extrapolate to larger time scales. This calls for a concise modeling strategy on how to extrapolate the regional estimates to long time scales, relevant to the Kyoto protocol (>5 yr). The best approach would seem to use models of biological processes and fossil fuel emission that are constrained by parameters that are optimized from data obtained during campaigns like CERES. Our intention is to analyze the current dataset carefully with the aim of identifying an optimum observational strategy for a regional long-term approach. For 2007, such a strategy in the same region is planned to obtain a full year’s carbon balance with a similar high spatial and temporal resolution as in the current experiment. A 20-yr high-resolution dataset of weather variables at 8-km resolution is

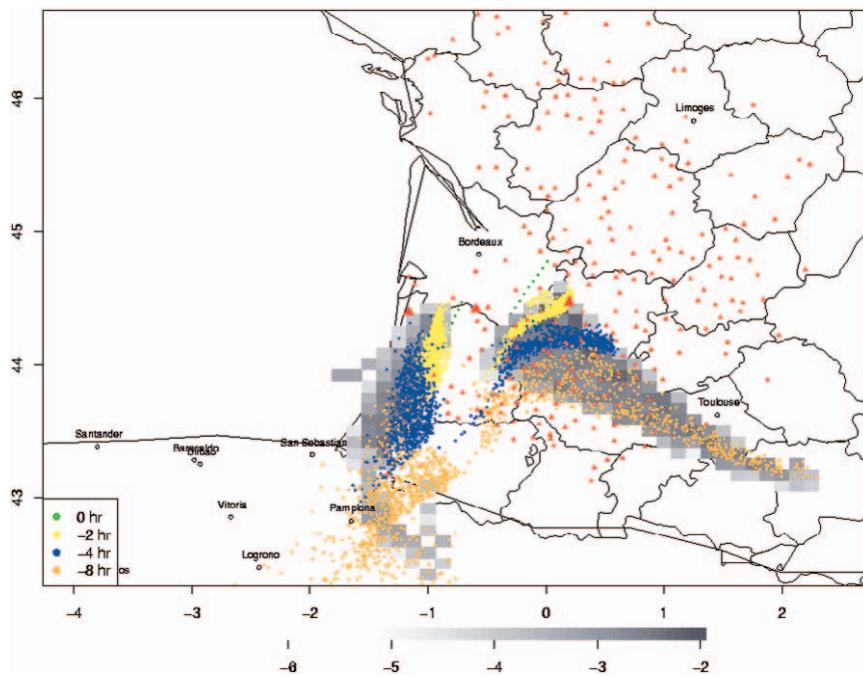


FIG. 7. STILT forecast of the concentration footprints based on Aladin on 26 May 1200 UTC forecast. The strong north–south footprint is for the measurement at Biscarrosse; the more inland footprint pictures the source are of the Marmande observations.

available to extrapolate even further back in time, to account for changes in land management and cropping techniques (Habets et al. 1999). CERES has shown that it is feasible to obtain a consistent dataset of surface and airborne observations of the fluxes and concentrations of CO₂. The availability of operational forecast tools has greatly helped our planning up to the point that we only had to cancel one flight due to bad weather conditions. We were also able to update flight plans on the basis of the predictions of the mesoscale model. The data obtained during CERES are only a first step to improve our understanding of the interaction between land use and the carbon cycle at the regional scale. After an initial period of analysis the data will be made available to interested partners. (More information on the experiment and progress of the analysis can be found on <http://carboregional.mediasfrance.org/index>.)

ACKNOWLEDGMENTS. A complex experiment like CERES draws on the resources and aid of many people. We particularly like to express our gratitude to the ATC of Saucats and Franczal, the staff at Saucats airport, the staff of SAFIRE (F. Monjauze and J.-F. Bourdinot) for coordinating the aircraft operations, the farmers who were kind enough to host our equipment, the Centre d'Essais en Vol for using their wind profiles and meteorological data, Medias France for hosting the Web site, and the many people in the field who performed the field observations. We would also like to thank the CNRM/4M and TRAMM teams who ran the central site under the responsibility of D. Legain, O. Garouste, and O. Traulle. The regional forecasters from Bordeaux and Toulouse helped us in planning the flights. J.-L. Champeaux provided the vegetation maps. S. Petitcol helped in setting up our two headquarters in Bordeaux and Toulouse. A. Zaldei and A. Matese (IBIMET-CNR) are thanked for their assistance with Sky Arrow, and P. Amico (Iniziativa Industriali Italiane), the pilot of the plane, is thanked for his relentless efforts in flying the flux plane at low altitudes. The help of the DP/service of Météo-France team for preparing the Aladin fields and the trajectories used during the Lagrangian IOPs is gratefully acknowledged. We gratefully acknowledge the thoughtful comments of two reviewers on an earlier draft of this manuscript. This work was executed as part of the CarboEurope-Integrated Project, supported by the European Commission through contract GOCE-CT2003-505572.

REFERENCES

- André, J.-C., J.-P. Goutorbe, and A. Perrier, 1986: HAPEX—MOBILHY: A hydrologic atmospheric experiment for the study of water budget and evaporation flux at the climatic scale. *Bull. Amer. Meteor. Soc.*, **67**, 138–144.
- Andreae, M. O., and Coauthors, 2001: Transport of biomass burning smoke to the upper troposphere by deep convection in the equatorial region. *Geophys. Res. Lett.*, **28**, 951–954.
- Aubinet, M., and Coauthors, 2000: Estimates of the annual net carbon and water exchange of forests: The EuroFlux methodology. *Adv. Ecol. Res.*, **30**, 113–176.
- Bélaïr, S., P. Lacarrère, J. Noilhan, V. Masson, and J. Stein, 1998: High-resolution simulation of surface and turbulent fluxes during HAPEX-MOBILHY. *Mon. Wea. Rev.*, **126**, 2234–2253.
- Bougeault, P., J. Noilhan, P. Laccarrère, and P. Mascart, 1991: An experiment with an advanced surface parameterization in the mesobeta-scale model. Part I: Implementation. *Mon. Wea. Rev.*, **119**, 2358–2373.
- Champeaux, J.-L., H. Fortin, and K.-S. Han, 2005: Spatio-temporal characterization of biomes over sw of France using SPOT/VEGETATION and Corine Land Cover datasets. *Proc. IEEE International Geoscience and Remote Sensing symposium*, Seoul, Korea, IEEE, 1295–1298.
- Crawford, T. L., R. J. Dobosy, R. T. McMillen, C. A. Vogel, and B. B. Hicks, 1996: Air-surface exchange measurement in heterogeneous regions: Extending tower observations with spatial structure observed from small aircraft. *Global Change Biol.*, **2**, 275–285.
- Curtis, P. S., P. J. Hanson, P. Bolstad, C. Barford, J. C. Randolph, H. P. Schmid, and K. B. Wilson, 2002: Biomertic and eddy covariance based estimates of annual carbon storage in the five eastern North American deciduous forests. *Agric. For. Meteorol.*, **113**, 3–19.
- de Arellano, J. V.-G., B. Gioli, F. Miglietta, H. J. J. Jonker, H. Klein Baltink, R. W. A. Hutjes, and A. A. M. Holtslag, 2004: Entrainment process of carbon dioxide in the atmospheric boundary layer. *J. Geophys. Res.*, **109**, D18110, doi:10.1029/2004JD004725.
- Denning, A. S., D. A. Randall, G. J. Collatz, and P. J. Sellers, 1996: Simulations of terrestrial carbon metabolism and atmospheric CO₂ in a general circulation model. Part 2: Spatial and temporal variations of atmospheric CO₂. *Tellus*, **48B**, 543–567.
- Dolman, A. J., R. Ronda, F. Miglietta, and P. Ciais, 2005: Regional measurement and modeling of carbon balances. *The Carbon Balance of Forest Biomes*, H. Griffiths and P. J. Jarvis, Eds., Garland Science/BIOS Scientific Publishers, 93–108.

- Gerbig, C., J. C. Lin, S. C. Wofsy, B. C. Daube, A. E. Andrews, B. B. Stephens, P. S. Bakwin, and C. A. Grainger, 2003: Toward constraining regional-scale fluxes of CO₂ with atmospheric observations over a continent: 2. Analysis of COBRA data using a receptor-oriented framework, *J. Geophys. Res.*, **108**, 4757, doi:10.1029/2003JD003770.
- Gioli, B., and Coauthors, 2003: Comparison of tower and aircraft-based eddy correlation fluxes at five sites in Europe. *Agric. For. Meteorol.*, **127**, 1–16.
- Gurney, K., and Coauthors, 2002: Towards robust regional estimates of CO₂ sources and sinks using atmospheric transport models. *Nature*, **415**, 626–630.
- Habets, F., and Coauthors, 1999: The ISBA surface scheme in a macroscale hydrological model applied to the HAPEX-Mobilhy area. Part I: Model and database. *J. Hydrol.*, **217**, 75–96.
- Hall, F. G., 2001: Introduction to special section: BOREAS III. *J. Geophys. Res.*, **106** (D24), 33 511–33 516.
- Janssens, I. A., and Coauthors, 2003: Europe's biosphere absorbs 7–12% of anthropogenic carbon emissions. *Science*, **300**, 1538–1542.
- Kaminski, T., P. J. Rayner, M. Heimann, and I. G. Enting, 2001: On aggregation errors in atmospheric transport inversions. *J. Geophys. Res.*, **106** (D5), 4703–4715.
- Körner, C., 2003: Slow in, rapid out—Carbon flux studies and Kyoto targets. *Science*, **300**, 1242–1243.
- Laubach, J., and H. Fritsch, 2002: Convective boundary layer budgets derived from aircraft data. *Agric. For. Meteorol.*, **111**, 237–263.
- Lin, J. C., and Coauthors, 2003: A near-field tool for simulating the upstream influence of atmospheric observations: The Stochastic Time-Inverted Lagrangian Transport (STILT) model. *J. Geophys. Res.*, **108**, 4493, doi:10.1029/2002JD003161.
- , and Coauthors, 2004: Measuring fluxes of trace gases at regional scales by Lagrangian observations: Application to the CO₂ Budget and Rectification Airborne (COBRA) study. *J. Geophys. Res.*, **109**, 15304, doi:10.1029/2004JD004754.
- Lloyd, J., and Coauthors, 2001: Vertical profiles, boundary layer budgets, and regional flux estimates for CO₂ and its ¹³C/¹²C ratio and for water vapor above a forest/bog mosaic in central Siberia. *Global Biogeochem. Cycles*, **15**, 267–284.
- Noilhan, J., and P. Lacarrère, 1995: GCM gridscale evaporation from mesoscale modeling. *J. Climate*, **8**, 206–223.
- Peylin, P., D. Baker, J. Sarmiento, P. Cias, and P. Bousquet, 2002: Influence of transport uncertainty on annual mean and seasonal inversions of atmospheric CO₂ data. *J. Geophys. Res.*, **107**, 4385, doi:10.1029/2001JD000857.
- Rödenbeck, C., S. Houweling, M. Gloor, and M. Heimann, 2003: CO₂ flux history 1982–2001 inferred from atmospheric data using a global inversion of atmospheric transport. *Atmos. Chem. Phys.*, **3**, 1919–1964.
- Schmitgen, S., P. Ciais, H. Geiss, D. Kley, A. Voz-Thomas, B. Neiniger, M. Bäumle, and Y. Brunet, 2004: Carbon dioxide uptake of a forested region in southwest France derived from airborne CO₂ and CO observations in a Lagrangian budget approach. *J. Geophys. Res.*, **109**, D14302, doi:10.1029/2003JD004335.
- Sellers, P. J., F. G. Hall, G. Asrar, D. E. Strelbel, and R. E. Murphy, 1988: The First ISLSCP Field Experiment (FIFE). *Bull. Amer. Meteor. Soc.*, **69**, 22–27.
- Styles, J. M., and Coauthors, 2002: Estimates of regional surface carbon dioxide exchange and carbon and oxygen isotope discrimination during photosynthesis from concentration profiles in the atmospheric boundary layer. *Tellus*, **54B**, 768–783.
- Valentini, R., and Coauthors, 2000: Respiration as the main determinant of carbon balance in European forests. *Nature*, **404**, 861–865.